N O T I C E

THIS DOCUMENT HAS BEEN REPRODUCED FROM MICROFICHE. ALTHOUGH IT IS RECOGNIZED THAT CERTAIN PORTIONS ARE ILLEGIBLE, IT IS BEING RELEASED IN THE INTEREST OF MAKING AVAILABLE AS MUCH INFORMATION AS POSSIBLE

NASA

Technical Memorandum 82104

Magnetic Space-Based Field Measurements

R. A. LANGEL

MARCH 1981

National Aeronautics and
Space Administration

Goddard Space Flight Center
Greenbelt, Maryland 20771

MAGNETIC SPACE-BASED FIELD MEASUREMENTS

R.A. Langel

The near-earth magnetic field is a complex combination of fields from outside the earth, fields from the core of the earth and fields from the crust of the earth. Furthermore, the first two mentioned sources are time varying. Magnetic field measurements from space have proven to be the only practical way to obtain timely, global surveys. Early measurements, commencing with the Sputnik and Vanguard spacecraft, measured only the magnitude of the field due to the extreme difficulty of making accurate vector measurements. The Magsat spacecraft, operable from November 2, 1979 through June 11, 1980, obtained the first truly accurate, global, vector magnetic survey. The attitude accuracy of 20 arc-seconds was achieved by the use of two star cameras and a very accurate sun-sensor supplemented by a pitch gyro and an optical system to transfer the spacecraft attitude to the location of the vector magnetometer at the end of the boom.

Measurements from Magsat, and earlier spacecraft, have been utilized to map both the earth's core fields and the fields arising in the geologically interesting crust of the earth. The standard model of the core field is of the same form today as that developed by Gauss in 1939. It consists of a scalar potential represented by a spherical harmonic series. Models of the crustal field are relatively new. The first global map appeared in the literature in 1975. Mathematical representation is achieved in localized areas by arrays of dipoles appropriately located in the earth's crust.

Besides the obvious use for navigation, measurements of the earth's field are utilized in diverse fields such as mapping of charged particles in the magnetosphere, studying fluid properties in the earth's core, inferring the electrical conductivity of the upper mantle and delineating regional scale geologic features.

INTRODUCTION

The near-earth magnetic field contains contributions from three sources: the earth's core, the earth's crust, and external current systems in the earth's ionosphere and beyond. By far the largest in magnitude is the field from the core, or the "main" field. Nearly dipolar in nature, the strength of the main field is more than 50,000 nT (nanotesla) as the poles and near 30,000 nT at the equator. Its variation with time ("secular" variation) is slow, with a maximum of about 1% per year. External current systems are time varying on a scale of seconds to days and can vary in magnitude from a fraction to thousands of nanoteslas. These current systems are located in a cavity-like region surrounding the earth, known as the "magnetosphere." Although always present the strength and location of these currents vary considerably between periods of magnetic quiet, defined as times when the temporal variation is small, and periods of magnetic disturbance when the temporal variations become large.

Prior to the satellite era the earth's magnetic field was (and still is) monitored by means of permanent magnetic observatories that measure the ambient field continuously (Figure 1), and by periodically repeating measurements at selected sites. Field surveys are necessary to fill in the spatial gaps between observatories and repeat sites. Such surveys were first conducted by early mariners and land surveyers. Edmund Halley made a sea voyage during 1689-1700 expressly to survey the magnetic field over the oceans. In 1701 he published the first chart of the magnetic declination in the region of the Atlantic Ocean; in the following year he extended his chart to the Indian Ocean and to the sea near China.

In addition to land and sea surveys some aircraft have been especially adapted for the measurement of magnetic fields. Such surveys have usually, although not always, measured only the scalar magnitude of the field. Many countries have been surveyed in their entirety, some more than once. In addition to their obvious value for modeling the earth's main field, such surveys are particularly useful for mapping the anomaly field at low altitude and, as a result, have been conducted by the oil and mineral exploration industry on a local scale.

Satellite measurements of the geomagnetic field began with the launch of Sputnik 3 in May 1958 and have continued sporadically in the intervening years. Table 1 is a list of spacecraft that have made significant contributions to our understanding of the near-earth geomagnetic field. Each had its own limitations, ranging from a lack of global coverage caused by the absence of on-board tape recorders to limited accuracy due either to instrumental shortcomings or to ambient spacecraft fields. Prior to Magsat, only the polar orbiting OGO 2, 4, and 6 (POGO) satellites have provided a truly accurate, global geomagnetic survey. These satellites operated between 1965 and 1971; their alkali vapor magnetometers provided global measurements of the field magnitude approximately every 1/2 second over an altitude range of about 400 to 1500 km.[1,2]

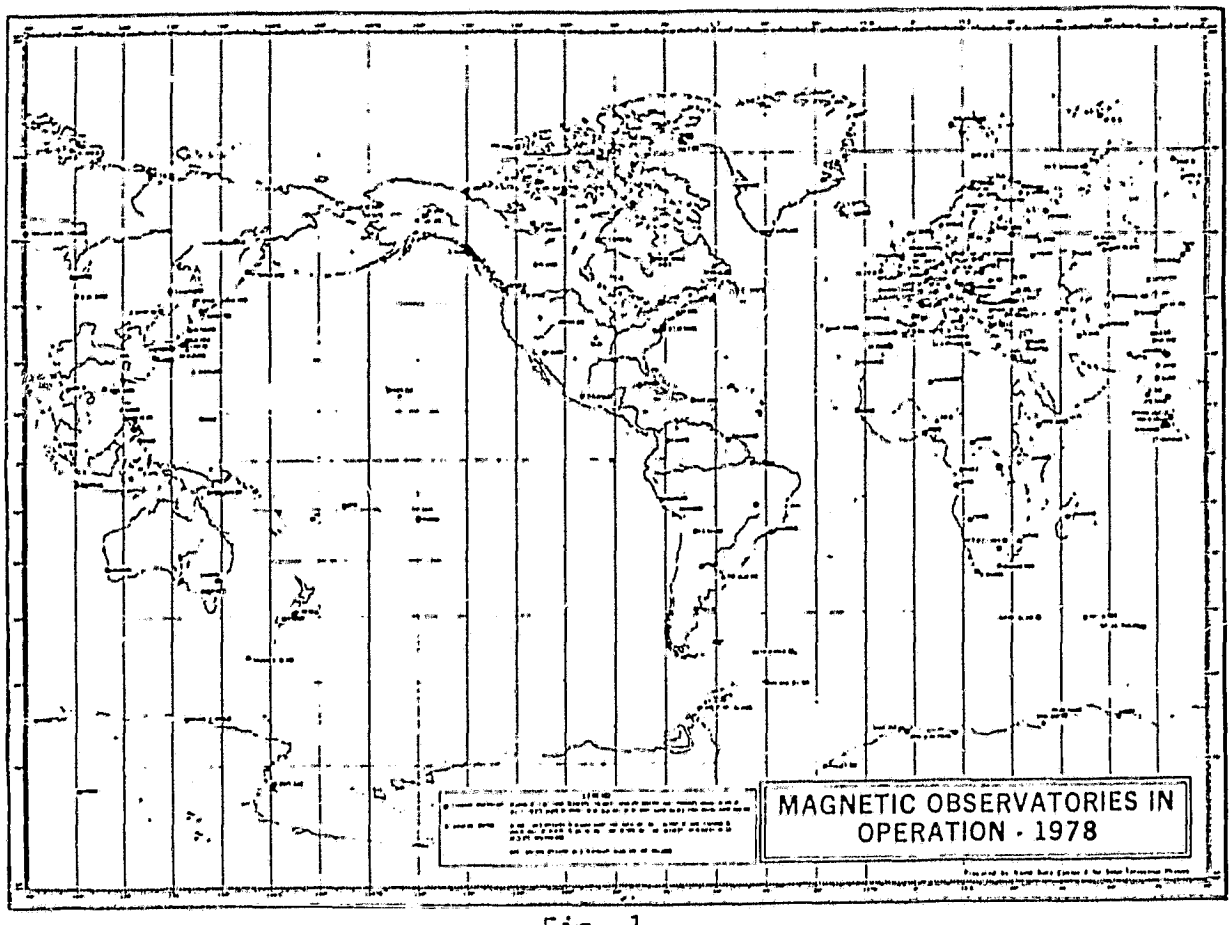

Fig. 1

Table 1

SATELLITES THAT HAVE MEASURED THE NEAR-EARTH GEOMAGNETIC FIELD

Satellite	*Inclination (degs)*	*Altitude Range (km)*	*Dates*	*Instrument*	*Approximate Accuracy (nT)*	*Coverage*
Sputnik 3	65	440 – 600	5/58 – 6/58	Fluxgates	100	USSR
Vanguard 3	33	510 – 3750	9/59 – 12/59	Proton	10	Near ground station*
1963-38C	Polar	1100	9/63 – 1/74	Fluxgate (1-axis)	30 – 35	Near ground station
Cosmos 26	49	270 – 403	3/64	Proton	Unknown	Whole orbit
Cosmos 49	50	261 – 488	10/64 – 11/64	Proton	22	Whole orbit
1964-83C	90	1040 – 1089	12/64 – 6/65	Rubidium	22	Near ground station
OGO-2	87	413 – 1510	10/65 – 9/67	Rubidium	6	Whole orbit
OGO-4	86	412 – 908	7/67 – 1/69	Rubidium	6	Whole orbit
OGO-6	82	397 – 1098	6/69 – 7/71	Rubidium	6	Whole orbit
Cosmos 321	72	270 – 403	1/70 – 3/70	Cesium	Unknown	Whole orbit
Azur	103	384 – 3145	11/69 – 6/70	Fluxgate (2-axis)	Unknown	Near ground station
Triad	Polar	750 – 832	9/72 – present	Fluxgate	Unknown	Near ground station

*"Near ground station" indicates no on-board recorder. Data were acquired only when the spacecraft was in sight of a station equipped to receive telemetry.

MAGSAT

A new era in near-earth magnetic field measurements began with NASA's launch of Magsat in October 1979. Magsat was launched into an orbit with 96.76° inclination, 561 km apogee and 352 km perigee. The orbit was sun-synchronous in the twilight plane. The magnetic field was measured with both a cesium vapor and a fluxgate magnetometer. In order to achieve 6 nT accuracy in the component measurements it was required to measure the spacecraft attitude to 20 arc-seconds. This was accomplished by two star cameras on-board the spacecraft and a sun-sensor attached to the vector magnetometer. In order to eliminate the effect of spacecraft magnetic fields, the magnetometers were located at the end of a 3 meter boom. An optical system measured the attitude of the magnetometer relative to the star cameras.

Magsat remained in orbit until June 11. Figure 2 shows the decay of the orbit.

Magsat has provided the first truly global geomagnetic surveys since the POGO satellites and the very first global survey of vector components of the geomagnetic field. Designed with two major measurement tasks in view, Magsat provided a global vector survey of the main geopotential field and a lower altitude measurement of crustal anomalies.

Data from Magsat is being analyzed by a large number of investigators, some of whom are working cooperatively. Investigations are being carried out by scientists at the Goddard Space Flight Center (GSFC) and the U.S. Geological Survey (USGS), and by scientists selected in response to a NASA Announcement of Opportunity (AO). This report reflects mainly the work at GSFC. A total of 19 domestic and 13 foreign investigators were selected from responses to the AO.

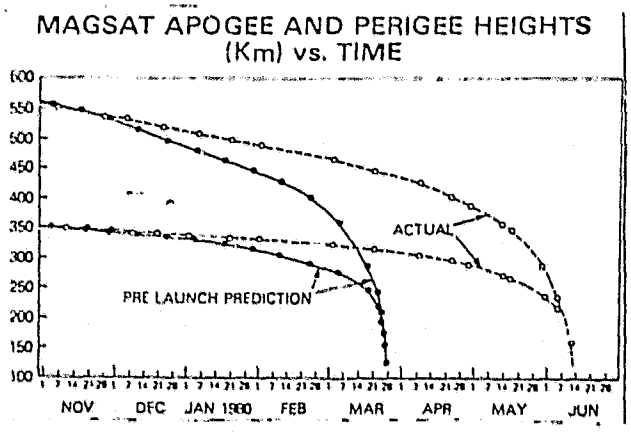

Fig. 2

GEOMAGNETIC FIELD MODELING

Geomagnetic field modeling derives the spherical harmonic potential function that best represents the main field of the earth in a least-squares sense. Theoretically such a potential function could be made to represent both the core and crustal fields exactly. In practice a restricted model must be chosen on practical grounds: the finite limitation on computer size and speed. Most researchers attempt only to represent the core field with a potential function and use alternate methods of describing the crustal fields.

One of the principal contributions of satellite magnetic field measurements to geomagnetism has been to make available a truly global distribution of data. Surface measurements are notably sparse, particularly in oceanic and remote regions. The problem is compounded by the secular variation in the main geomagnetic field which as was stated earlier, can amount to as much as 1% per year in some localities. This means that to represent the global geomagnetic field accurately at any given time (epoch), worldwide measurements must be made at times near that epoch, a feat only achieved by satellite observations, and even then only by the POGO and Magsat satellites with their on-board tape recorders and near-polar orbits. Accurate global representation of the secular variation itself would require periodic worldwide surveys. The POGO satellites accomplished one such survey and Magsat furnished another. These, together with existing surface data, permit accurate global representation of secular variation for the period beginning with OGO 2 until the demise of Magsat: roughly October 1965 through June 1980. Future satellite surveys will be needed for accurate global representations beyond the lifetime of Magsat.

Although POGO data were global and taken over a short time span, the limitation of measuring only the field magnitude resulted in some ambuguity in the field direction in spherical harmonic analyses based on POGO data alone.[3-6] This ambiguity has been removed by the acquisition of global vector data with Magsat. In deriving a spherical harmonic model, the presence of large amplitude external fields would contaminate the results. For this reason only data from selected magnetically quiet periods is chosen. Of the Magsat data currently available for analysis, November 5 and 6 showed the lowest value of magnetic activity indices. Plots of the data indicated that these days were indeed very quiet magnetically. Accordingly, a selection of 15,206 data points from those days was used to derive the first geomagnetic field model from Magsat, designated MGST (6/80)[7].

This model fits the selected data with the mean and standard deviations as follows:

Component	Mean Deviation (nT)	Standard Deviation (nT)
Scalar magnitude	0.1	8.2
B_r	2.5	6.5
$B\theta$	-0.1	7.6
$B\phi$	0.5	7.4

The fit to the data is very good with deviations mainly due to a combination of fields from unmodeled external and crustal sources.

Magsat data has now been combined with other selected data to derive a preliminary model valid for the period 1960 to 1980. In order to represent the long term, or secular, variation of the main field, first, second and third derivation of some of the spherical harmonic coefficients were derived. Besides Magsat, POGO data, data from 147 magnetic observatories and selected repeat station and shipborne data were included. The resulting spherical harmonic coefficients, designated GSFC(9/80) are given in Table 2. Table 3 summarizes the statistics for GSFC(9/80) and, for comparison, our best pre-Magsat model (PMAG(6/80)), the recently published[8] model used in the British and U.S. Naval 1980 world magnetic charts, WC80, the model[9] utilized in the USGS 1975 world charts, and the MGST(6/80) model. Note:

1. The GSFC(9/80) model represents the Magsat data almost as well as does MGST(6/80) even though GSFC(9/80) is applicable for 20 years while MGST(6/80) is for a single epoch.

2. PMAG(7/80) represents Magsat data substantially better than other pre-Magsat models.

3. Both PMAG(7/80) and GSFC(9/80) represent the POGO data better than either WC80 or ACW75.

It is not really fair to compare the representation of surface data between models since some models include solution for the observatory anomaly fields at the surface.

Figure 3 shows how these procedures allow accurate representation of observatory data during the time span of the data utilized in the model. The data plotted is for the observatory at Amberley. The three measured components, yearly averages, are plotted with X, Y, Z symbols. The predicted field from GSFC(9/80), taking the observatory anomaly solution into account, is represented by the indicated lines. The model represents the measured field very well for 1960.5-1975.5 but increasingly diverge for years prior to 1960. This is typical for prediction outside the range of data included in the spherical harmonic derivation. For some observatories the divergence is much greater than for Amberley while for some it is not as large. The predictive

Table 2

n	m	g_n^m	h_n^m	$\dot{g}_n^m$	$\dot{h}_n^m$	$\ddot{g}_n^m$	$\ddot{h}_n^m$	$\dddot{g}_n^m$	$\dddot{h}_n^m$
1	0	-29437.9	0.0	20.41	0.0	-0.403	0.0	-0.0151	0.0
1	1	-1957.4	5506.7	9.03	-8.06	-0.224	0.579	-0.0078	0.021
2	0	-1995.7	0.0	-19.53	0.0	0.294	0.0	0.0064	0.0
2	1	3027.7	-2129.4	4.78	-14.74	0.240	-1.440	0.0014	-0.047
2	2	1612.9	1445.6	9.16	27.02	0.347	-0.307	0.0033	-0.013
3	0	1282.2	0.0	4.51	0.0	0.062	0.0	0.0193	0.0
3	1	-2290.4	3335.5	-3.55	5.57	0.069	-1.109	0.0114	-0.030
3	2	1651.4	270.9	2.19	1.64	0.176	-0.078	0.0003	-0.002
3	3	852.9	-2351.5	-3.47	-6.62	0.573	-0.244	0.0130	-0.013
4	0	937.1	0.0	-2.20	0.0	-0.128	0.0	-0.0040	0.0
4	1	782.3	211.0	-2.44	3.66	-0.043	-0.120	-0.0032	-0.006
4	2	397.2	-2566.8	-10.09	1.09	-0.403	0.033	-0.0014	0.001
4	3	-414.6	59.4	-3.32	6.77	-0.132	0.554	-0.0009	0.012
4	4	1008.3	2588.0	-5.54	-2.73	-0.224	-0.096	-0.0059	-0.003
5	0	-217.1	0.0	-1.04	0.0	-0.080	0.0		
5	1	357.0	458.2	-0.96	3.30	-0.048	0.086		
5	2	261.5	1449.9	-0.73	-0.50	-0.092	-0.067		
5	3	-74.3	-1506.7	-4.81	-0.52	-0.136	0.093		
5	4	-161.5	-777.7	0.11	1.09	-0.015	-0.018		
5	5	-147.7	918	1.49	0.87	0.009	0.009		
6	0	49.1	0.0	0.75	0.0	0.039	0.0		
6	1	65.0	-14.6	-0.04	0.03	-0.031	0.024		
6	2	42.0	934	3.49	-1.20	0.074	-0.037		
6	3	-191.4	70.9	-2.70	-0.56	-0.012	-0.067		
6	4	3.9	-442.9	0.44	0.11	0.018	0.048		
6	5	14.1	-1.9	1.78	0.56	0.039	0.003		
6	6	-107.1	17.5	1.14	2.72	0.078	0.041		
7	0	71.0	0.0	0.08	0.0	0.0	0.0		
7	1	-58.1	83.2	-0.34	-1.44	0.0	0.0		
7	2	1.3	-27.1	0.05	-0.03	0.0	0.0		
7	3	20.1	-5.5	0.45	0.15	0.0	0.0		
7	4	-13.0	15.9	0.94	0.59	0.0	0.0		
7	5	0.8	17.9	0.17	-0.37	0.0	0.0		
7	6	10.8	-24.0	-0.20	0.03	0.0	0.0		
7	7	-2.7	-9.9	0.09	0.54	0.0	0.0		
8	0	18.9	0.0	0.60	0.0	0.0	0.0		
8	1	7.2	7.5	0.08	-0.05	0.0	0.0		
8	2	0.9	-17.7	0.22	-0.30	0.0	0.0		
8	3	-10.4	3.2	0.08	-0.09	0.0	0.0		
8	4	-7.1	-22.4	-0.24	-0.34	0.0	0.0		
8	5	4.0	9.4	-0.15	0.31	0.0	0.0		
8	6	3.7	16.3	0.53	-0.54	0.0	0.0		
8	7	7.1	-13.4	-0.48	-0.67	0.0	0.0		
8	8	-1.3	15.2	-0.26	0.05	0.0	0.0		
9	0	5.2	0.0	-0.31	0.0	0.0	0.0		
9	1	-10.7	-21.8	-0.17	0.06	0.0	0.0		
9	2	1.0	16.0	-0.34	0.09	0.0	0.0		
9	3	-12.0	6.9	-0.72	-0.24	0.0	0.0		
9	4	9.2	-4.7	-0.12	-0.19	0.0	0.0		
9	5	-3.9	-7.5	-0.27	-0.27	0.0	0.0		
9	6	-1.1	4.5	-0.04	-0.02	0.0	0.0		
9	7	7.1	-10.8	0.27	-0.05	0.0	0.0		
9	8	1.5	-5.3	-0.00	-0.28	0.0	0.0		
9	9	-5.0	2.1	-0.45	0.15	0.0	0.0		
10	0	8.3	0.0	-0.12	0.0	0.0	0.0		
10	1	-4.1	1.0	-0.39	-0.07	0.0	0.0		
10	2	2.7	-0.1	0.04	-0.04	0.0	0.0		
10	3	-5.5	2.6	-0.09	0.05	0.0	0.0		
10	4	-1.6	5.5	0.01	-0.06	0.0	0.0		
10	5	5.2	-4.3	-0.01	-0.01	0.0	0.0		
10	6	2.6	-1.3	-0.19	-0.14	0.0	0.0		
10	7	1.3	-1.1	0.18	-0.12	0.0	0.0		
10	8	2.4	4.4	0.07	0.14	0.0	0.0		
10	9	3.2	-0.6	0.09	-0.09	0.0	0.0		
10	10	-0.3	0.2	0.03	-0.05	0.0	0.0		
11	0	2.3	0.0	-0.02	0.0	0.0	0.0		
11	1	-0.6	1.1	0.03	-0.03	0.0	0.0		
11	2	2.3	2.4	-0.03	-0.01	0.0	0.0		
11	3	2.1	-2.1	-0.13	-0.02	0.0	0.0		
11	4	0.3	-2.3	0.06	-0.05	0.0	0.0		
11	5	-0.4	0.4	-0.02	-0.02	0.0	0.0		
11	6	-0.5	-0.1	-0.01	-0.02	0.0	0.0		
11	7	1.4	-3.5	-0.01	-0.19	0.0	0.0		
11	8	1.5	-0.2	-0.11	0.05	0.0	0.0		
11	9	-0.8	-0.7	0.09	0.15	0.0	0.0		
11	10	1.9	-1.7	-0.10	-0.06	0.0	0.0		
11	11	3.4	-0.1	0.08	-0.29	0.0	0.0		
12	0	-2.0	0.0	-0.04	0.0	0.0	0.0		
12	1	-0.2	0.5	-0.03	0.00	0.0	0.0		
12	2	0.5	0.5	0.11	-0.00	0.0	0.0		
12	3	-0.3	2.0	-0.02	-0.08	0.0	0.0		
12	4	-0.2	-1.9	-0.06	-0.13	0.0	0.0		
12	5	-1.1	0.5	0.04	-0.04	0.0	0.0		
12	6	-0.3	0.2	0.03	-0.00	0.0	0.0		
12	7	0.1	0.2	0.04	-0.03	0.0	0.0		
12	8	0.2	-0.3	-0.01	-0.10	0.0	0.0		
12	9	0.5	-0.5	-0.06	-0.09	0.0	0.0		
12	10	0.5	0.6	0.01	-0.09	0.0	0.0		
12	11	0.8	0.0	0.09	-0.07	0.0	0.0		
12	12	0.3	-0.1	-0.03	-0.01	0.0	0.0		
13	0	0.5	0.0	0.02	0.0	0.0	0.0		
13	1	0.2	0.3	0.03	-0.07	0.0	0.0		
13	2	0.2	0.2	-0.05	-0.01	0.0	0.0		
13	3	0.0	-1.9	-0.00	-0.03	0.0	0.0		
13	4	0.2	0.8	-0.00	-0.09	0.0	0.0		
13	5	0.5	-1.0	0.01	-0.03	0.0	0.0		
13	6	0.2	0.2	0.03	-0.06	0.0	0.0		
13	7	0.3	-1.2	0.03	-0.06	0.0	0.0		
13	8	-0.5	0.2	-0.00	-0.01	0.0	0.0		
13	9	0.2	-0.7	-0.01	-0.01	0.0	0.0		
13	10	-0.4	-0.1	0.00	-0.02	0.0	0.0		
13	11	-0.2	-0.5	0.02	-0.04	0.0	0.0		
13	12	-0.0	0.4	0.00	-0.03	0.0	0.0		
13	13	0.6	-0.4	0.07	-0.01	0.0	0.0		

Table 3

DATA TYPE	STATISTIC TYPE	MODEL MGST(6/80)	AWC75	WC80	PMAG(7/80)	GSFC(9/80)
Magsat						
scalar	r.m.s.	8.2	138.9	118.7	82.2	10.1*
	mean	0.1	60.0	-20.6	-24.0	-1.6
	std. dev.	8.2	125.2	115.9	78.8	10.0
X-component***	r.m.s.	7.6	100.1	91.7	65.5	9.0
	mean	-0.2	24.7	-33.4	-27.9	-1.4
	std. dev.	7.6	97.9	85.5	59.3	8.9
Y-component***	r.m.s.	7.4	79.6	59.7	62.7	8.5
	mean	0.1	-1.3	-1.1	-1.6	-0.1
	std. dev.	7.4	79.6	59.7	62.7	8.5
Z-component***	r.m.s.	6.9	157.4	113.2	98.3	9.2
	mean	-2.5	24.9	20.9	8.4	-2.6
	std. dev.	6.5	155.4	111.3	97.9	8.8
POGO						
scalar	r.m.s.	--	69.8	121.6	6.7	6.9
	mean	--	43.8	21.3	37.7	-0.15
	std. dev.	--	54.4	119.8	3.5	6.9
Observatory			1967-1974	1974-1977	1960-1977	1960-1977
X-component	r.m.s.	--	284.5	302.7	37.6**	39.9**
	mean	--	-24.7	41.5	18.7	5.6
	std. dev.	--	283.4	299.9	-0.06	39.6
Y-component	r.m.s.	--	352.8	240.9	18.7	19.3
	mean	--	-48.3	-15.8	16.5	0.4
	std. dev.	--	349.5	240.5	-0.05	19.3
Z-component	r.m.s.	--	515.6	584.3	16.5	15.2
	mean	--	-23.7	-71.0	26.9	-0.11
	std. dev.	--	515.0	579.9	0.52	15.2

*Magsat residuals to GSFC(9/80-1) were taken including the MGST(6/80) external terms with GSFC(9/80-1) because the Magsat data used to derive GSFC(9/80-1) was corrected for that external field.

**PMAG(7/80) and GSFC(9/80-1) include estimates of observatory "anomalies" which are taken into account when computing residuals.

***Does not include data at latitudes greater than 50^{0} or less than -50^{0}.

capability of GSFC(9/80) seems to be acceptable back to about 1955 or 1956, a range of 4-5 years outside the data span of the model.

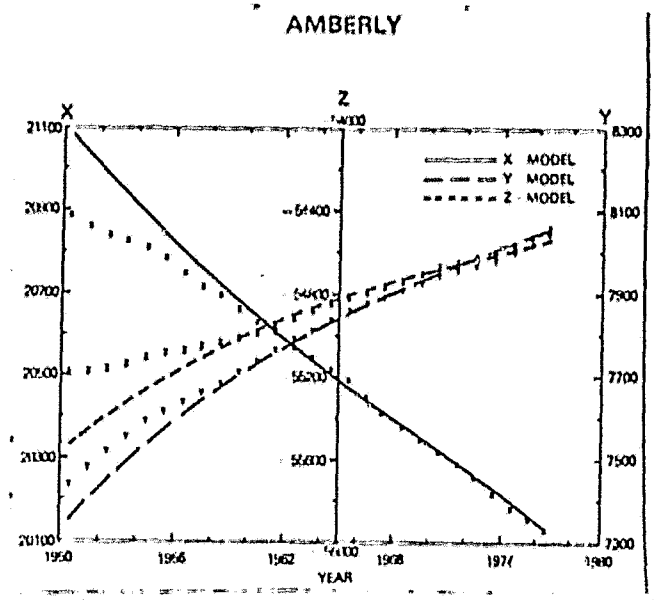

Fig. 3 Comparison of Measured Data With Model at an Observatory

CRUSTAL MAGNETIC ANOMALY STUDIES

A crustal magnetic anomaly is the residual field after estimates of the core and external fields have been subtracted from the measured field. An anomaly map is a contour map of the measured average anomaly field at the altitude of the data. Anomaly maps have been derived from aeromagnetic and shipborne data for many years and used in the construction of geologic/geophysical models of the crust. Investigations with aeromagnetic and shipborne magnetic data have mainly concentrated on the very localized anomalies associated with small-scale geologic features and localized mineralization. However, in the past few years there has been an increased interest in studies of the broad-scale anomalies that appear in regional compilations of aeromagnetic and shipborne data.[10-14] Satellite anomaly maps are of recent origin and describe only the very broadest scale anomalies. Aeromagnetic and shipborne anomaly maps have usually been interpreted assuming a flat earth and a constant ambient field over the region of interest. Because of the extremely large scale of satellite-derived anomalies, both of these assumptions become invalid, thus necessitating development of new analysis techniques.

Originally, it was thought impossible to detect fields of crustal origin in satellite data. However, while analyzing data from the POGO satellites, Regan et al.[15] discovered that the lower-altitude data contained separable fields caused by crustal anomalies, Figure 4, thus opening the door to a new class of investigations. None of the satellites shown in Table 1 was designed for solid earth studies, yet results from the POGO satellites have demonstrated the capability of mapping broad-scale anomalies. Although the map of Regan et al. was partially contaminated

by "noise" from magnetospheric and ionospheric fields, the reality and crustal origin of several of the anomalies defined by the map were clearly demonstrated. More recently Langel et al.[16] have compared a POGO-derived anomaly map with upward-continued aeromagnetic data from western Canada. Figure 5 shows the results of that comparison. The two maps are in substantial agreement, demonstrating further both the reality and crustal origin of the anomalies.

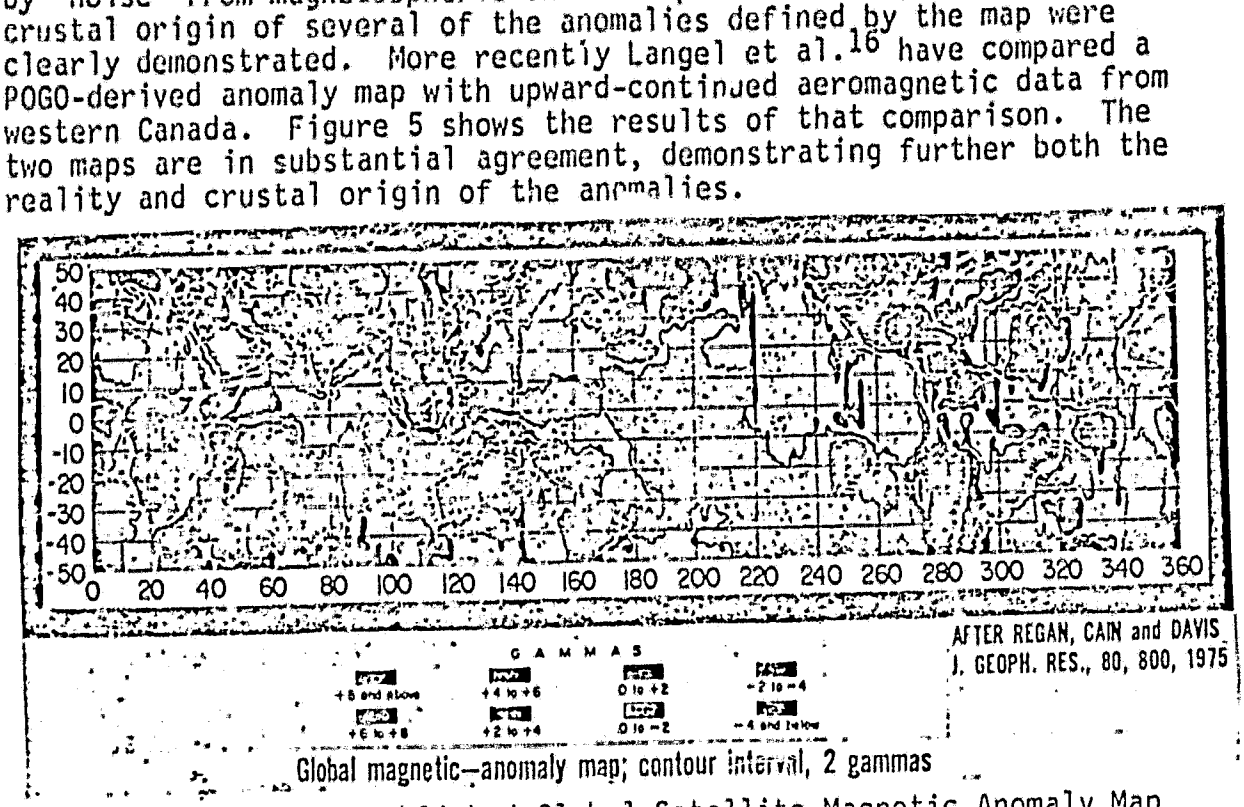

Fig. 4 The First Published Global Satellite Magnetic Anomaly Map

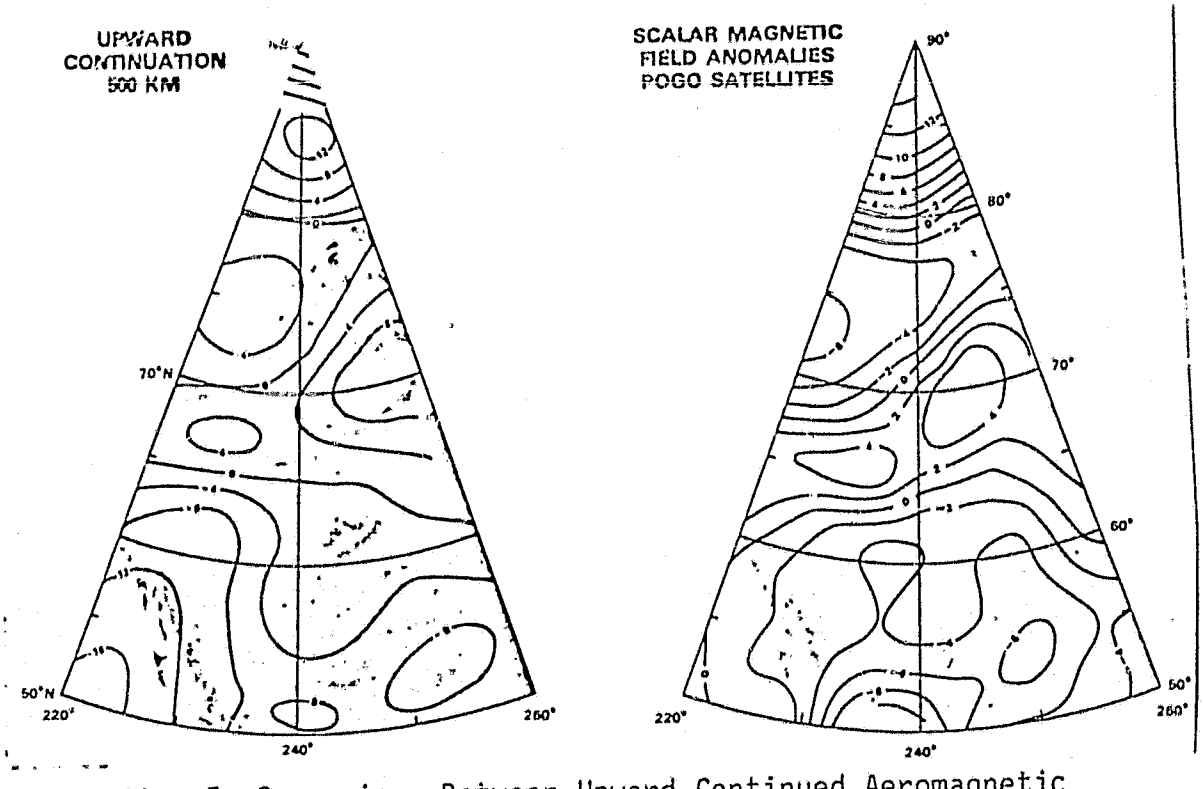

Fig. 5 Comparison Between Upward Continued Aeromagnetic Data and POGO Anomaly Data

Average maps can be misleading because the average satellite altitude is not everywhere the same. To overcome this and to provide the capability of representing the anomalies on maps of differing scale and projection, a mathematical representation of the anomaly field is derived. This consists of an array of dipoles equally spaced over the earth's surface and oriented along the ambient main field. The strength of the dipole is calculated to give a "best fit" to the measured anomaly data, selected from suitable quiet times and filtered so as to minimize external field contributions.

Using these techniques, a global map has been derived from POGO data and is shown in Figure 6. Although we have not yet reduced it to common altitude, a preliminary scalar anomaly map has been derived from Magsat data (Figure 7). It's features agree well with those seen by POGO (Figure 6) but more details are resolved because of the lower altitude. Figure 7 included Magsat data through February of 1980.

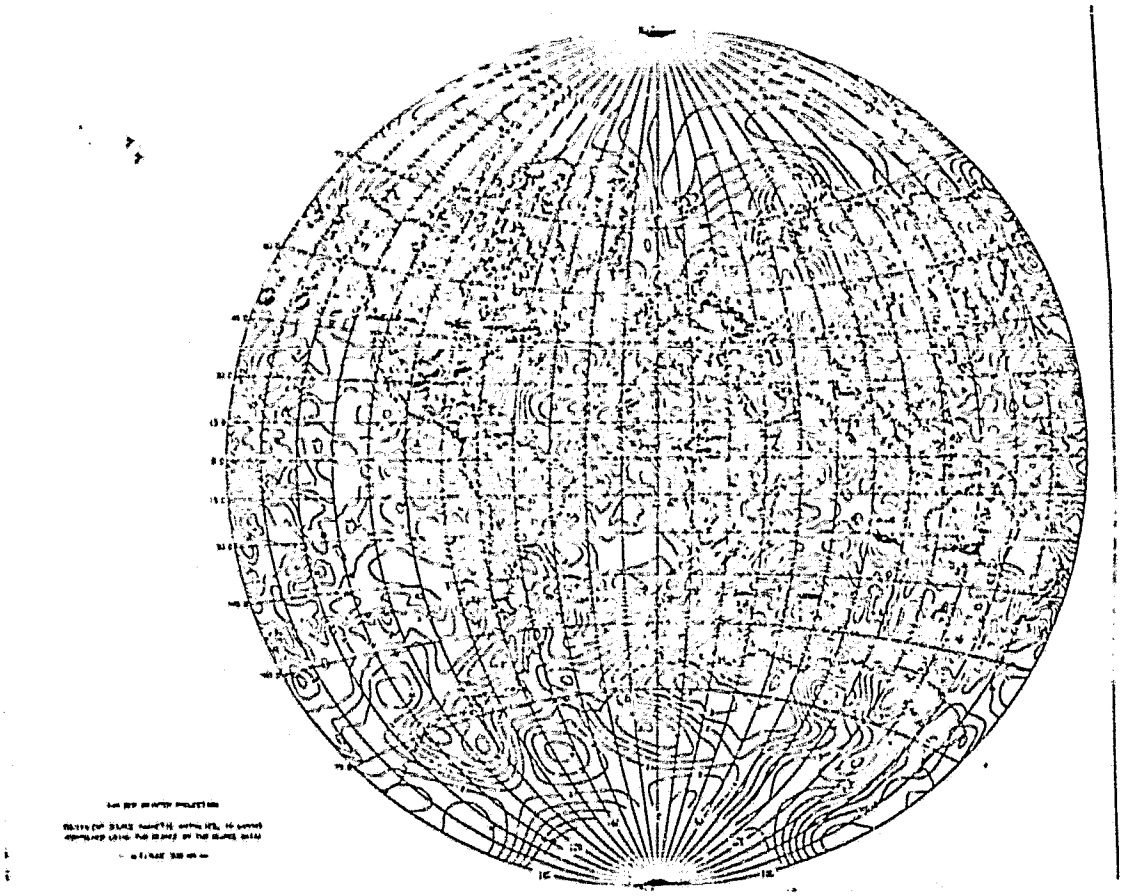

Fig. 6 Global Anomaly Map from POGO Data
Reduced to 500 km Altitude

Future maps with later data will be at still lower altitudes giving even better resolution. This is illustrated in Figure 8 which shows how resolution increases as altitude decreases. The anomaly map is from POGO data. The solid line shows a common track location for OGO 4 and Magsat. The scalar residual fields from the two spacecraft are shown on the right. The OGO-4 altitude was 414-420 km whereas the Magsat data, acquired the day prior to re-entry, are at 187-191 km. Examination of the plots show clearly the existence of anomalous fields in the Magsat data which are only hinted at in the POGO data.

Magsat has also acquired vector data. Analysis of the data is considerably more time consuming than for scalar data and no anomaly maps have been prepared. Figure 9 shows one full orbit of data. The plots are of residuals to a thirteenth degree and order field model. Anomalous fields are clearly present in the scalar data at the top. In the X and Y components, external fields are present as indicated by the fluctuating residuals near the poles. Two anomalies, however, are clearly present in the vector data. In the center of the plot at about 5-10° north latitude is a low in scalar field and a corresponding low in the X and Z components. This is the Bangui or Central African anomaly. Just to the north of Bangui, at about 60°N latitude (at 4:42:39 UT) is another low in scalar field with corresponding lows evident in the X and Z component. This anomaly is over northern Scandanavia.

For geologic studies such anomaly maps must be inverted to a description of the magnetic properties of the crustal rocks. Such inversions are not unique; constraints from other data sources will be required in their interpretation. As a first step in such modeling, traditional equivalent source methods, adapted for the case of a spherical earth with changing field inclination, have been applied to the United States[17] and Australia[18]. This technique assumes a constant 40 km

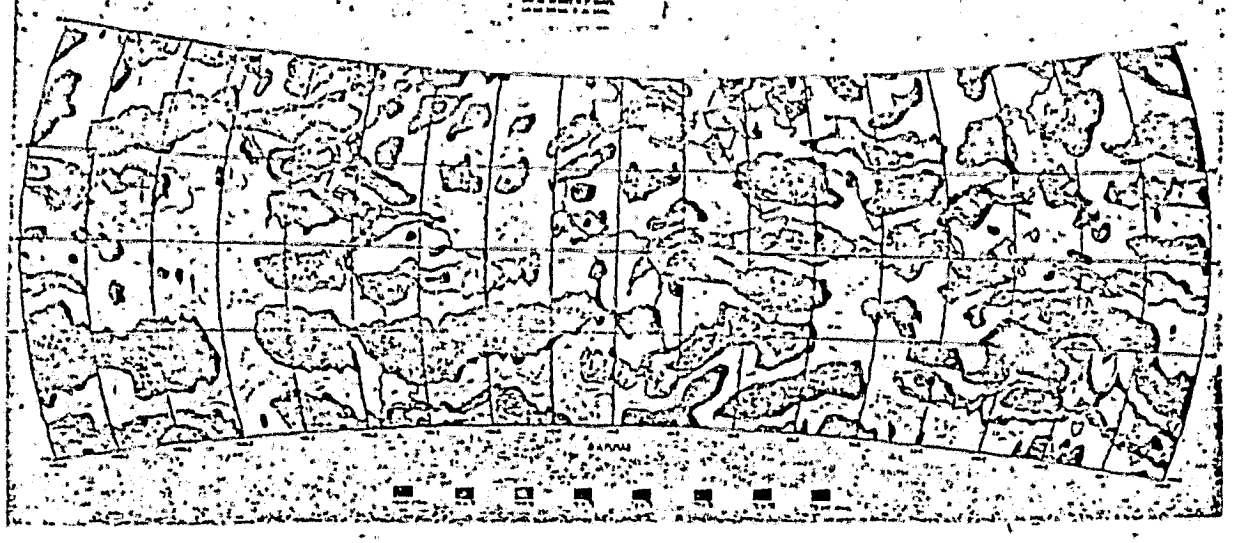

Fig. 7 First (Preliminary) Scalar Anomaly Map from Magsat Data

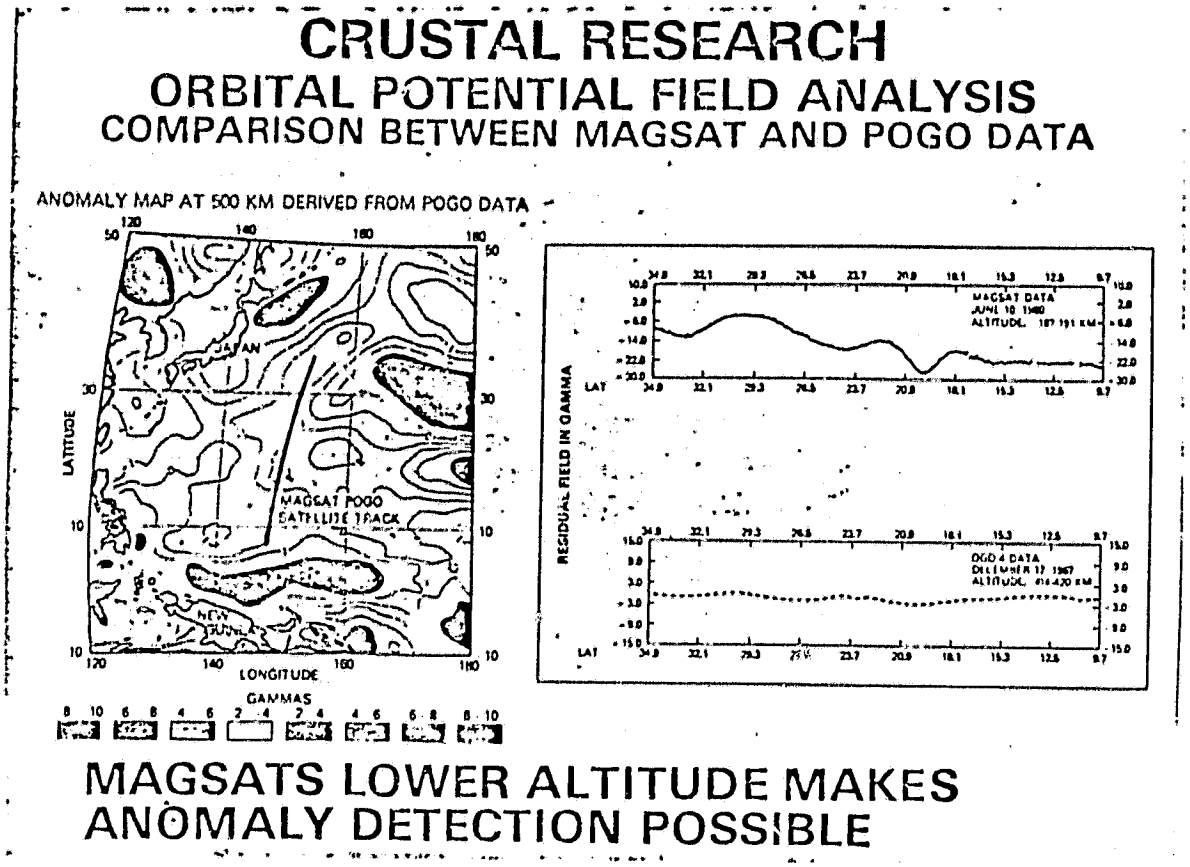

Fig. 8

thickness of the magnetic crust and derives the magnetization in such a crust that would cause the anomalies seen at the spacecraft. All of the anomalous field is assumed to be zero. The results for the United States are shown in Figure 10. In many regions known geologic features are clearly outlined (e.g., the Basin and Range Province, Colorado Plateau, Rio Grande Rift, Michigan Basin, and Mississippi Embayment) whereas some features are notable by the absence of magnetic features (e.g., the mid-continent gravity high). It will be some years before these maps are fully understood and interpreted, but they promise to shed new light on the geology of the deep crust.

Anomaly maps, or even magnetization maps, are not an end in themselves. The object of these efforts is to derive models of the crust and upper mantle for large-scale regions of the globe. There are many kinds of models; their common purpose is to generalize observations and prediction. Through synthesis of particular models, complex models of crustal geologic systems are built up in terms of structural and compositional variations and the movements of material and energy. Conclusions can then be drawn about the evolution of regions that lead to inferences about the distribution of natural resources.

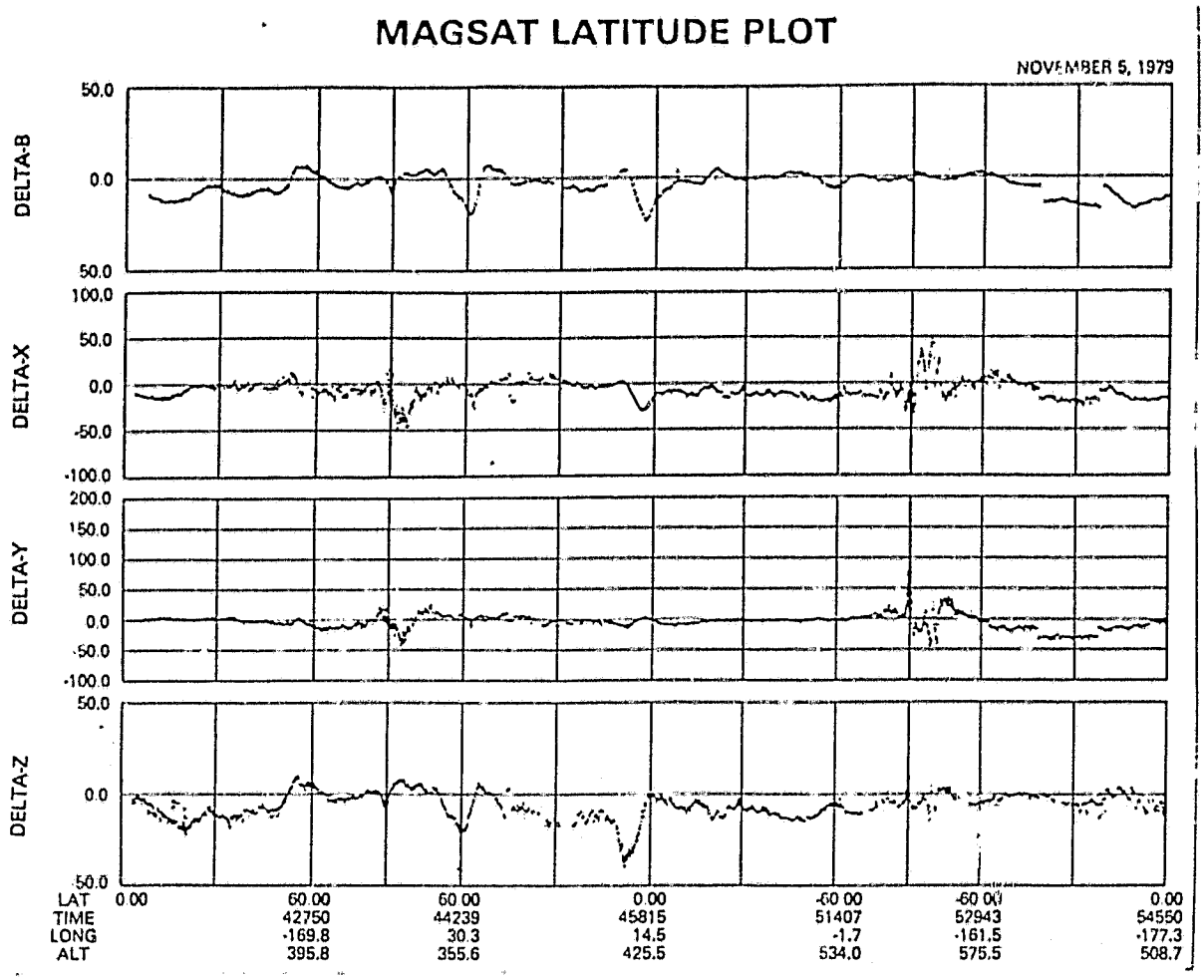

Fig. 9 Magnitude and Component Data from Magsat after Removal of Field From a Spherical Harmonic Model

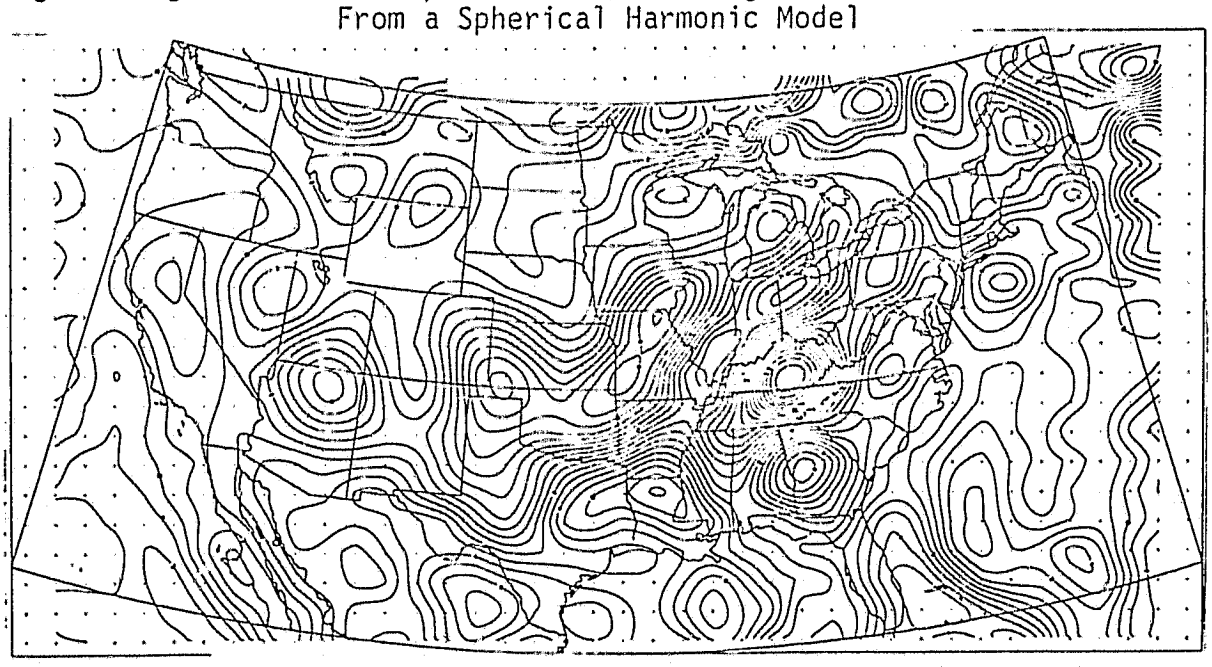

Fig. 10 Equivalent Bulk Magnetization from POGO Data Assuming a Constant-Thickness Magnetic Crust of 40 km. Units are emu/cm^3x10^4.

INVESTIGATIONS OF THE INNER EARTH

Man has directly penetrated only a few kilometers of the 6378 km distance to the earth's center. Information about the inner earth must be obtained by indirect methods such as seismology and measurements of the gravity and magnetic fields.

Combining Magsat data with POGO and near-surface surveys will permit more accurate determination of the secular variation of the core field. This variation will be used to study properties of the fluid motions in that core; in turn, appropriate magnetohydrodynamic constraints will be investigated to determine if they can aid in better modeling the secular variation.

When they are time-varying, magnetospheric fields result in induced fields within the earth because of the finite conductivity of the earth. The characteristics of these induced fields are determined by the properties of the materials in the earth's mantle (i.e., composition, temperature). At present the limiting factor in determining a precise conductivity profile within the earth, with adequate spatial resolution, is the accuracy possible in determining the external and induced fields. Magsat vector measurements, together with surface data will be used for a more accurate analysis than was previously possible.

CONCLUSION

Satellite-based magnetic field measurements make global surveys practical for both field modeling and for the mapping of large-scale crustal anomalies. They are the only practical method of accurately modeling the global secular variation. Magsat is providing a significant contribution, both because of the timeliness of the survey and because its vector measurement capability represents an advance in the technology of such measurements.

Data from Magsat is available for any interested user through the National Space Sciences Data Center at GSFC.

With the success of Magsat, future missions should take two courses. Field modeling requires periodic surveys, but not low-altitude measurements as required for crustal studies. On the other hand, further advances in satellite crustal studies will rest on NASA's ability to orbit magnetometers at still lower altitudes, concepts for which are still in the state of discussions as to their feasibility.

ACKNOWLEDGEMENTS

I wish to thank all members of the Magsat team for making possible the acquisition and Analysis of these data. Program management at NASA Headquarters is in the able hands of Jim Murphy and Mark Settle. Although it is not feasible to name all those included, my special thanks go to Gil Ousley of GSFC and L.D. Eckard of APL for directing the effort that culminated in the successful construction, launch, and operation of Magsat; to Mario Acuna and W.H. Farthing for the design and oversight of the magnetometers; to John Berbert and Earl Beard of GSFC and Don Berman of Computer Sciences Corporation and their colleagues for their efforts at data preparation; and to Locke Stuart and his team at GSFC for their successful organization of and interface with the Magsat investigators. Finally, I particularly appreciate the encouragement, advice, and general support of Gil Mead and Lou Walter of the GSFC Applications Directorate and Barbara Lueders of the GSFC Geophysics Branch.

REFERENCES

1. J.C. Cain and R.A. Langel, "Geomagnetic Survey by the Polar-Orbiting Geophysical Observatories," World Magnetic Survey 1957-1969, (A.J. Zmuda, ed.) IAGA Bulletin No. 18, 1979.

2. R.A. Langel, "Near Earth Magnetic Disturbance in Total Field at High Latitude, I. Summary of Data from OGO 2, 4, and 6," J. Geophys. Res. 79, pp. 2363-2371, 1974.

3. G.E. Backus, "Nonuniqueness of the Esternal Geomagnetic Field Determined by Surface Intensity Measurements," J. Geophys. Res., 75, pp. 6339-6341, 1970.

4. L. Hurwitz and D.G. Knapp, "Inherent Vector Discrepancies in Geomagnetic Main Field Models Based on Scalar F," J. Geophys. Res., 74, pp. 3009-3013, 1974.

5. D.P. Stern and J.H. Bredekamp, "Error Enhancement in Geomagnetic Models Derived from Scalar Data," J. Geophys. Res., 80, pp. 1776-1782, 1975.

6. F.J. Lowes, "Vector Errors in Spherical Harmonic Analysis of Scalar Data," Geophys. J. Roy. astron. Soc., 42, pp. 637-651, 1975.

7. R.A. Langel, R.H. Estes, G.D. Mead, E.B. Fabiano and E.R. Lancaster, "Initial Geomagnetic Field Model from Magsat Vector Data," Geophys. Res. Lett., 7, pp. 793-796, 1980.

8. F.S. Barker and D.R. Barraclough, "World Magnetic Chart Model for 1980," E@S, trans. A.G.U., 61, 453, 1980.

9. N.W. Peddie and E.B. Fabiano, "A Model of the Geomagnetic Field for 1975," J. Geophys. Res., 81, pp. 1539-2542, 1976.

10. L.C. Pakiser and I. Zietz, "Transcontinental Crustal and Upper Mantle Structure," Rev. Geophys., 3, pp. 505-520, 1965.

11. I. Zietz, E.R. King. W. Geddes and E.G. Lidiak, "Crustal Study of a Continental Strip from the Atlantic Ocean to the Rocky Mountains," Geolog. Soc. Am. Bull., 77, pp. 1427-1448, 1966.

12. R.T. Shuey, D.R. Schellinger, E.H. Johnson and L.G. Alley, "Aeromagnetics and the Transition Between the Colorado Plateau and the Basin Range Province," Geology, 1, pp. 107-110, 1973.

13. D.H. Hall, "Long Wavelength Aeromagnetic anomalies and Deep Crustal Magnetization in Manitoba and North Western Ontario, Canada," J. Geophys, 40, pp. 403-430, 1974.

14. A.A. Kruithovskaya and I.K. Paskevich, "Magnetic Model for the Earth's Crust under the Ukrainian Shield," Canadian J. Earth Sci., 14, pp. 2718-2728, 1977.

15. R.D. Regan, J.C. Cain and W.M. Davis, "A Global Magnetic Anomaly Map," J. Geophys. Res., 80, pp. 794-802, 1975.

16. R.A. Langel, R.L. Coles and M.A. Mayhew, "Comparisons of Magnetic Anomalies of Lithospheric Origin as Measured by Satellite and by Airborne Magnetometers over Western Canada," Canadian J. Earth Sci., XVII, pp. 876-887, 1980.

17. M.A. Mayhew, "Satellite Derived Equivalent Magnetization of the United States," (in preparation, 1979).

18. M.A. Mayhew, B.D. Johnson and R.A. Langel, "Magnetic Anomalies at Satellite Elevation over Australia," Earth Planet. Sci. Lett., 51, 189-198, 1980.